Pergamon

Tetrahedron, Vol. 53, No. 8, pp. 2697-2716, 1997

0040-4020/97 $17.00 + 0.00

PII: S0040-4020(97)00045-8

HETERONUCLEAR NOE ANALYSIS OF BILIRUBIN SOLUTION CONFORMATION AND INTRAMOLECULAR HYDROGEN BONDING

Thomas Dörner, Bernd Knipp and David A. Lightner*

Chemistry Department, University of Nevada, Reno, NV 89557 USA

Abstract. $^{1}H\{^{1}H\}$-Homonuclear and $^{13}C\{^{1}H\}$-heteronuclear NOE (Nuclear Overhauser Effect) experiments carried out on bilirubin analogs (**1-5**) in $CDCl_3$ and in $CDCl_3$-$(CD_3)_2SO$ solutions indicate that the carboxylic acid groups and dipyrrinone lactams and/or pyrroles are linked by intramolecular hydrogen bonding. Nonbonded C-H to H-C and N-H to H-N, and N-H to CO_2H distances were calculated from the NOE data and confirm that the bilirubins adopt a folded, ridge-tile shape in solution.

INTRODUCTION

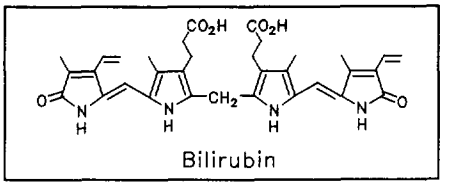

Bilirubin

Bilirubin is a water-insoluble pigment produced in adult humans at a rate of about 300 mg per day by heme catabolism.[1,2] It occurs only in vertebrates and is clinically important for several reasons:[2,3] its accumulation in blood and extravascular tissue is a useful sign of disease, usually liver disease; it can cause irreversible neurologic damage; it is involved in the formation of gallstones; and it may be an important radical-intercepting antioxidant.[4] In addition, bilirubin and its glucuronides have been studied extensively as paradigmatic models for hepatic glucuronidation and for carrier-mediated hepatic uptake and excretion.[5]

Bilirubin is conformationally flexible in solution, but one conformation is significantly more stable than all the others: a folded ridge-tile structure with intramolecular hydrogen bonds between the pyrrole and lactam functions of the dipyrrinone halves and the propionic carboxyl (or carboxylate) groups (Fig. 1).[6-8] Although bilirubin can form helical conformers, they are of relatively high energy, and the linear conformation (above) is especially high energy.[8-11] The ridge-tile conformation is the only one that has been observed in crystals of bilirubin[6,7] and its carboxylate salts.[12] Early spectroscopic studies, particularly NMR, have been supported by energy calculations and strongly suggest that hydrogen-bonded ridge-tile conformers also prevail in solution, even in the dipolar protophilic solvent dimethyl sulfoxide.[8,13-15] Individual ridge-tile conformers of bilirubin are chiral and both enantiomers occur in solution,[16] interconverting rapidly[13] via a succession of non-planar intermediates in which the hydrogen bonding network is never completely broken.[8,11] The energetically most favored ridge-tile conformation (with interplanar angle, θ ~100°) is *not* rigid, however; it is flexible. Small, low energy rotations about the C(9)-C(10) and C(10)-C(11) bonds cause θ to open or close somewhat, while

maintaining hydrogen bonding (Fig. 1).[8] However, large rotations break hydrogen bonds and lead to energetically disfavorable conformations. Such large bond rotations are associated with the interconversion of mirror image ridge-tile conformations — a dynamic process that occurs at an experimentally-determined rate of ~5.4 sec^{-1} at 37°C[8] over an experimentally-determined barrier of ~18-20 kcal/mole.[17] The picture of bilirubin structure is thus one of *flexible* enantiomeric *ridge-tile shapes* that *interconvert rapidly* at room temperature.

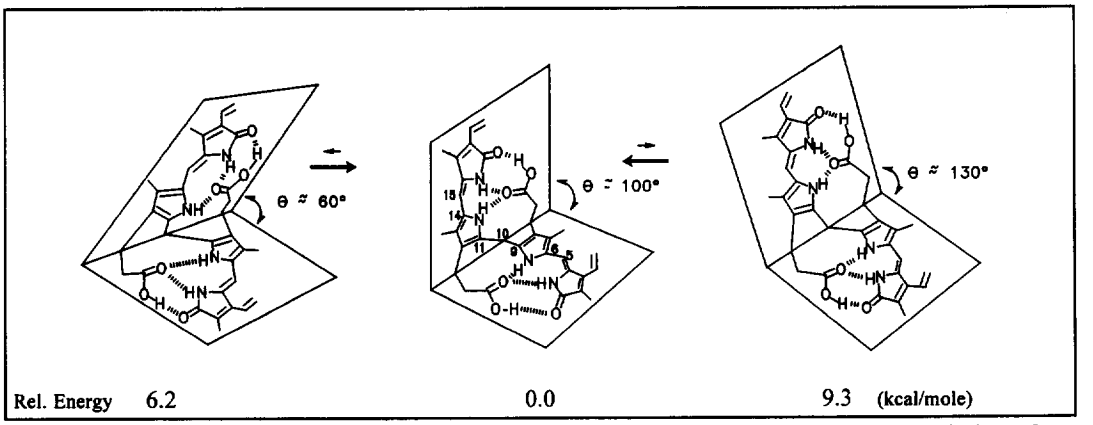

FIGURE 1. Lepidopterous action in ridge-tile bilirubin (middle) illustrating its flexibility. Only one enantiomer is shown. Low energy rotations about the C(9)-C(10) and C(10)-C(11) bonds cause the dipyrrinones to flutter, *i.e.*, the ridge-tile expands or contracts (θ increases or decreases). Further expansion leads to even higher energy stretched or linear conformers; further contraction leads to even higher energy helical (porphyrin-like) conformers. Energies from SYBYL molecular mechanics (ref. 8).

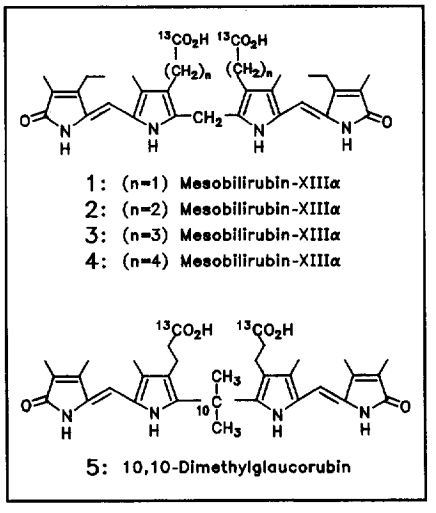

Bilirubin analogs with shorter (**1**) and longer (**3** and **4**) alkanoic acid chains[18] are also believed to be able to engage in conformation-determining intramolecular hydrogen bonding.[19] In such pigments, the interplanar angle (θ, Fig. 1) of the ridge-tile is thus predicted to be smaller (in **1**) or larger (**3** and **4**) than that of bilirubin or mesobilirubin (**2**) with propionic acid chains. And when the central methylene bridge at C(10) is substituted with a *gem*-dimethyl group (**5**), internal steric interactions are thought to cause a widening of the interplanar angle.[20] The purpose of the following study is to detect and explore the importance of intramolecular hydrogen bonding in **1** and **3-5** by $^{1}H\{^{1}H\}$-homonuclear[21] and $^{13}C\{^{1}H\}$-heteronuclear NOE[22] studies, and to reconfirm earlier studies on **2**.[15]

RESULTS AND DISCUSSION

Synthesis. The total syntheses of unlabelled bilirubin pigments **1-4** have been described previously,[18] as have the syntheses of ^{13}C-labelled **2**[23,24] and **5**.[23] Preparation of ^{13}C-labelled acetic, butanoic and pentanoic acid analogs **1**, **3** and **4** generally followed the route described for the synthesis of ^{13}C-labelled **2**.[23] The key ^{13}C-labelled precursors were (1) pyrrole acetic acid **30**, prepared by a modified Fischer pyrrole synthesis from pentane-2,4-dione which had been alkylated using [1-^{13}C] bromoacetic acid ester, and (2) pyrrole nitriles **18-20**

SYNTHETIC SCHEME

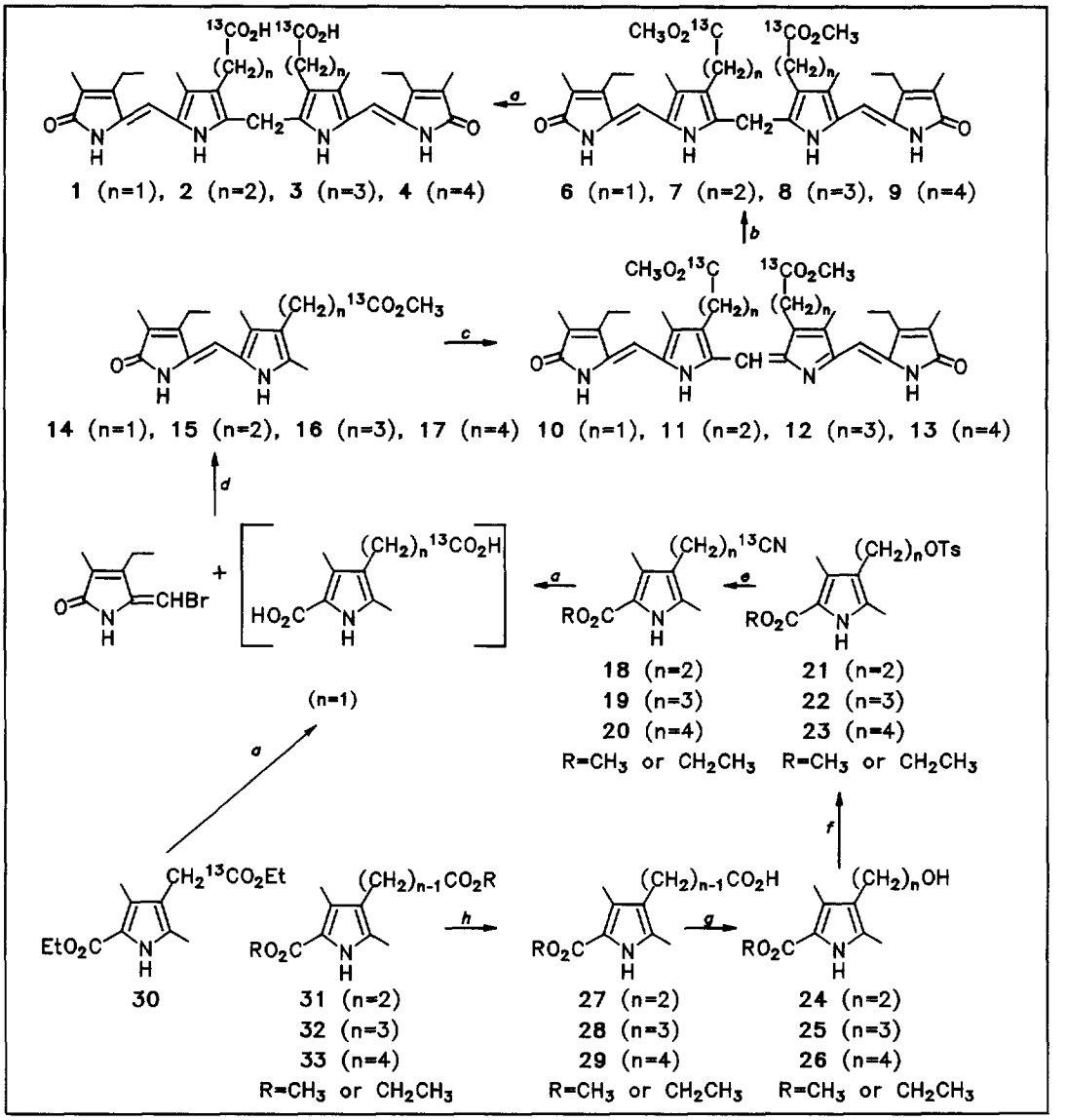

[a] Excess NaOH; [b] $NaBH_4/CH_3OH$; [c] *p*-chloranil/HCO_2H-$CHCl_3/\Delta$; [d] CH_3OH/Δ; [e] $K^{13}CN/(CH_3)_2SO$; [f] *p*-toluenesulfonyl chloride/pyr.; [g] BH_3·THF; [h] 1 equiv. NaOH.

(Synthetic Scheme). The nitrile route, which was used to prepare homologated acids, involved introduction of the ^{13}C label using 99% enriched $K^{13}CN$. Convenient starting materials for this route were the lower homolog diesters (**31-33**) available from earlier work.[18] The diesters were selectively saponified in 88-97% yield to give the corresponding half-acids (**27-29**), which were reduced selectively using borane-tetrahydrofuran complex to give the corresponding alcohols (**24-26**) in 74-99% yield. The alcohols were then converted to the corresponding tosylates (**21-23**). Reaction with $K^{13}CN$ afforded ^{13}C-labelled nitriles **18-20** in 81-92% yield.

The latter were hydrolyzed in base to afford the corresponding diacids (65-83%), the key relay compounds used in preparing dipyrrinones **14-17** (in 63-67% yield) by condensation with a bromomethylenepyrrolinone as described previously.[18] The resulting dipyrrinone methyl esters (**14-17**) were converted to tetrapyrrole verdin esters **10-13** in 81-90% yield via oxidative coupling using *p*-chloranil.[18] The verdins were reduced smoothly by $NaBH_4$ in 81-90% yield to give the corresponding rubin diesters **6-9**, which were easily saponified to the desired rubin acids (**1-4**) in 82-90% yield.

Relaxation Times. Bilirubin and mesobilirubin are thought to be *monomeric* in chloroform on the basis of UV and NMR spectroscopy and ultracentrifugation sedimentation equilibrium studies.[1,17,25-28] The monomer is believed to adopt preferentially an intramolecularly hydrogen-bonded, flexible ridge-tile conformation (Fig. 1) with planar dipyrrinone units.[6-17,25-28] Dimethyl sulfoxide solutions are also monomeric,[13,25-29] with the conformation of the monomer similar to that in chloroform, except for the inclusion of solvent molecules in the hydrogen bonding matrix.[8] In contrast, bilirubin dimethyl ester is known to be *dimeric* in chloroform,[25-27] with self-association by dipyrrinone to dipyrrinone intermolecular hydrogen bonding.[13,25,28] In dimethyl sulfoxide, however, the solutions are monomeric.[13,26,29] To prepare for measuring the NOEs of **1-5**, **7** and **8**, T_1 relaxation times (Table 1) were determined for the ^{13}C-labelled carboxyl carbons. It may be noted that the acid carboxyl T_1 values measured in $CDCl_3$ are about one-half those of the dimethyl esters, as might be expected for carboxylic acid groups involved in intramolecular hydrogen bonding *vs* carbomethoxy groups that are less constrained by hydrogen bonding. Even small amounts of added $(CD_3)_2SO$ reduce T_1 of the CO_2H groups significantly, in keeping with earlier conclusions[13] that the conformation of bilirubin in $(CD_3)_2SO$ is similar to that in $CDCl_3$, but in $(CD_3)_2SO$ the "propionic CO_2H and CO_2CH_3 groups are tied to the nearest pyrrole NH and lactam groups via bound solvent molecules."[29]

TABLE 1. Carboxyl Chemical Shifts and Selective T_1 Relaxation Times for Mesobilirubins at 25°C.[a]

Pigment	Solvent	$\delta_{^{13}C}$ (ppm)	^{13}C T_1 (sec)
1 (n=1)	$CDCl_3$	177.72	3.9
2 (n=2)	$CDCl_3$	179.49	3.6
2 (n=2)	$CDCl_3$-$(CD_3)_2SO$ (90:10)	—	2.9
2 (n=2)	$CDCl_3$-$(CD_3)_2SO$ (80:20)	178.29	2.4
2 (n=2)	$CDCl_3$-$(CD_3)_2SO$ (70:30)	177.35	2.3
2 (n=2)	$(CD_3)_2CO$-$(CD_3)_2SO$ (67:37)	175.15	4.4
2 (n=2)	$(CD_3)_2SO$	173.96	2.4
3 (n=3)	$CDCl_3$	180.49	2.6
4 (n=4)	$CDCl_3$	180.20	3.0
5	$CDCl_3$	179.86	3.6
7 (diester)	$CDCl_3$	173.64	5.9
8 (diester)	$CDCl_3$	174.25	7.5

[a] Chemical shifts in δ (ppm) downfield from $(CH_3)_4Si$, ref. $CDCl_3$ (δ=77.0) or $(CD_3)_2CO$ (δ=29.92).

Analysis of NOE Results in $CDCl_3$ Solvent. A survey of homo and heteronuclear NOEs has been determined for bilirubin analogs **1-5**, with the most important NOEs shown in Tables 2 and 3. (N.B. The relative values of the NOEs are important for structure determination and not the absolute NOE numbers.) Our NOEs, obtained on a 500 MHz NMR, are somewhat lower than the values reported in the literature for bilirubin at 90 MHz,[25] and they are also somewhat lower than the preliminary values we had measured at 300 MHz NMR. Absolute NOEs depend crucially on the contribution of other relaxation pathways and for a given compound in a given solvent, they might even differ to some extent from sample to sample. We assume that the lower NOE values found at 500 MHz are due mainly to an increasing contribution of chemical shift anisotropy because the rate for this relaxation pathway increases with the square of the applied field. In all cases no significant $^{13}C\{^1H\}$-NOEs to the acid carbon were detected other than from the well-separated,[8,13,16-18,20,25,26] selectively-irradiated acid side-chain CH_2 protons and the acid OH, lactam NH or pyrrole NH protons.

TABLE 2. $^1H\{^1H\}$-Homonuclear and $^{13}C\{^1H\}$-Heteronuclear NOEs From Mesobilirubins at 25°C.

Rubin	Solvent	$^1H\{^1H\}$-Homonuclear NOEs[a]				$^{13}C\{^1H\}$-Heteronuclear NOEs[a]			
	irradiate: detect:	acid-H lact.-H	lact.-H acid-H	lact.-H pyrr.-H	pyrr.-H lact.-H	acid-H COOH	lact.-H COOH	pyrr.-H COOH	all H COOH
1	$CDCl_3$	~0[b]	~0[b]	~15	~5	~35[b]	~0	~0	~105
2	$CDCl_3$	2.8	2.2	22.2	20.3	34.0	3.6	1.8	89.6
2	$CDCl_3$[c]	3.7	3.0	15.9	14.8	28.7	3.2	2.0	79.7
2	$CDCl_3$[d]	e	e	e	e	33.0	4.0	2.2	91.4
2	$CDCl_3$ 90% $(CD_3)_2SO$ 10%	~0	~0	17.4	14.9	32.4	3.1	1.7	81.1
2	$CDCl_3$ 80% $(CD_3)_2SO$ 20%	−7.6[f]	<0[f]	12.4	10.0	25.8	e,f	e	85.0
2	$CDCl_3$ 70% $(CD_3)_2SO$ 30%	−5.0[f]	<0[f]	6.4	8.2	25.7	e,f	e	73.4
2	$(CD_3)_2CO$ 67% $(CD_3)_2SO$ 33%	−3.2[f]	~0	6.1	7.1	22.2	0.7[f]	0.1	83.1
2	$(CD_3)_2SO$	~0	~0	−7.2	−12.1	14.4	0.3	0.2	48.0
2[g]	$CDCl_3$	5.1	3.6	21.7	23.4	49.3	3.5	2.5	134.0
3	$CDCl_3$	~0	~0	12.9	17.4	38.6	4.3	2.3	77.0
4	$CDCl_3$	b,f	b,f	10.4	8.6	32.4[b]	e,f	2.7[h]	86.7
5	$CDCl_3$	3.9	6.6	17.8	19.5	34.0	3.6	1.8	92.1
5	$CDCl_3$[i]	4.3	5.0	16.0	17.4	34.6	3.2	1.5	93.2

[a] Values in %, as determined on a 500 MHz Varian Unity Plus NMR. Values < 1 are reported as ~0. [b] Exchange acid/residual water protons, therefore water peak was irradiated. [c] 0°C. [d] 37°C. [e] Not determined. [f] Saturation transfer. [g] Run on a 300 MHz GN-300. [h] Artifact? [i] 10 mm broad band probe.

(n=2) Mesobilirubin-XIIIα (2). $^1H\{^1H\}$-Homonuclear NOE experiments from **2** in $CDCl_3$ reveal a large NOE between the lactam (10.7 ppm) and the pyrrole (9.0 ppm) protons of the dipyrrinones (Table 2). The C(5) and C(15) olefinic protons (6.1 ppm) receive considerable NOEs from the C(3) and C(17) ethyl groups (-CH_2-, 2.5 ppm; -CH_3, 1.1 ppm) of the lactam ring as well as from the C(7) and C(13) methyl groups (2.1 ppm) (Table 3). Both of these sets of NOEs provide evidence for a *syn-Z* conformation of the dipyrrinone

units, or as shown in Fig. 1. This is consistent with earlier NOE experiments carried out by Navon and Kaplan[13,25] confirming the *syn-Z* stereochemistry for the dipyrrinones of bilirubin. However, because the exact conformation of both the lactam ethyl and the pyrrole methyl groups are not known, the relative values of their NOEs with the olefinic hydrogens at C(5) and C(15) cannot be used for determining an exact value of the C(4)-C(5)-C(6)-N and N-C(14)-C(15)-C(16) torsion angles. In addition to these NOEs, and in accord with earlier results for bilirubin,[13] we have also detected significant NOEs between the lactam and the acid protons (Table 2). Such NOEs are consistent with intramolecular hydrogen bonding between the COOH group of the propionic acid side chain from one half of the molecule and the lactam moiety (and probably also the pyrrole NH) of the other half of the molecule (and vice-versa), as expressed in the ridge-tile conformations of Fig. 1.

TABLE 3. Homonuclear $^1H\{^1H\}$-NOEs Associated with Lactam and Pyrrole Rings of Bilirubin Analogs.[a]

Rubin	Solvent	I	II	I/II[b]	III	IV	V	III/V[b]
	irradiate: detect:	lact. NH pyrr. NH	CH_2 (10) pyrr. NH		CH_2CH_3 CH (5,15)	CH_2CH_3 CH (5,15)	Pyrr. CH_3 CH (5,15)	
2	$CDCl_3$	22.2	3.4	6.5	20.0	3.1	10.7	1.9
2	$CDCl_3$ 90% $(CD_3)_2SO$ 10%	18.2	2.5	7.3	11.2	1.9	11.9	0.9
2	$CDCl_3$ 80% $(CD_3)_2SO$ 20%	12.4	2.1	5.8	[c]	[c]	[c]	[c]
2	$CDCl_3$ 70% $(CD_3)_2SO$ 30%	6.4	0.7	9.1	7.0	3.2	4.7	1.5
2	$(CD_3)_2CO$ 67% $(CD_3)_2SO$ 33%	6.1	2.5	2.4	~7[d]	1.1	~8[d]	~0.9[d]
2	$(CD_3)_2SO$	−7.2	−3.1	2.3	0.8	1.4	−6.7	–
3	$CDCl_3$	12.9	2.6	5.0	4.6–9.2[d]	2.1	10.5	0.4–0.9[d]
4	$CDCl_3$	10.4	2.1	5.0	6.1	1.9	9.2	0.7
5	$CDCl_3$	17.8	—	—	>13.5[e]	—	>14.5	0.9[d]

[a] Values in %, determined on a Varian Unity Plus 500 MHz NMR at 25°C. [b] Relative ratio of NOE values. [c] Not determined. [d] Not determined exactly due to accidental saturation of other peaks. [e] Methyl group.

$^{13}C\{^1H\}$-Heteronuclear NOE experiments show that the COOH carbon receives large NOEs from the acid OH protons (13.6 ppm) as well as from the CH protons of the propionic acid chain (Table 2). The NOE value from the acid OH protons amounts to 34%, about one third of the total NOE that the acid carbon receives. We have not attempted to determine NOEs quantitatively for the side chain proton because the broad and second order coupling patterns of these protons prevent us from knowing the extent of saturation of each of these protons in heteronuclear experiments. Therefore, such experiments would not make any real sense. In addition to the expected NOEs, the acid carbon also receives small but significant NOEs from the lactam NH proton as well as from the pyrrole NH proton. The NOE from the lactam proton, with a value of nearly 4%, is about twice as large as the NOE from the pyrrole proton. These NOEs indicate a relatively close spatial proximity between the propionic acid COOH carbons and the lactam and pyrrole protons. Such a close proximity of these nuclei is only possible between opposite halves of the molecule and is best explained by intramolecularly hydrogen-bonded conformations similar to those of Fig. 1. No other significant heteronuclear NOEs

to the acid carbon were detected. To determine whether there are temperature-dependent structural changes for **2** in $CDCl_3$, we carried out NOE studies at 0°C and at 37°C. At 0°C the values of most of the homo and heteronuclear NOEs decrease slightly, but the relative NOE values were unchanged. The slight decrease can be attributed to extended correlation times at 0°C. At 37°C, human body temperature, the NOE values showed no major changes. Therefore, it seems safe to assume a single fixed conformation of **2** within the temperature range 0° to 37°C.

(n=1) Mesobilirubin-XIIIα (1). Mesobilirubin **1** is very insoluble in chloroform. We were not able to detect NOEs between the residual water (which exchanges with the acid protons) and the lactam protons. We were also unable to detect NOEs from either the lactam protons or from the pyrrole protons to the acid carbon. We attribute this to the extremely low solubility of **1**, leaving smaller NOEs (below ≈5%) far below our detection level. Consequently, we could thus deduce no information about hydrogen bonding in **1**.

(n=3) Mesobilirubin-XIIIα (3). For the higher mesobilirubin homolog with a butanoic acid side chain (**3**), $^1H\{^1H\}$-homonuclear NOEs between the lactam protons and the pyrrole protons are found to be of the same order of magnitude (Table 2) as for **2**, which has propionic acid side chains — again indicating a *syn-Z* geometry in the dipyrrinones. In contrast, no significant NOEs between the lactam and the acid protons were detected. $^{13}C\{^1H\}$-heteronuclear NOE experiments indicate significant NOEs from the lactam and the pyrrole protons to the side chain acid carbon CO_2H. The NOE values are comparable to those of **2**. The NOE from the acid OH proton to the acid CO_2H carbon of **3** is somewhat higher than observed in **2**, possibly indicating a slightly different geometry. The results show that in **3**, hydrogen bonding between the lactam and pyrrole NH protons and the acid carbonyl oxygen still takes place. However, we did not find any evidence of hydrogen bonding between the acid OH hydrogens and the lactam ring carbonyl oxygens. Nevertheless, our results indicate that the conformation of **3** is close to that of **2**, a ridge-tile structure.

(n=4) Mesobilirubin-XIIIα (4). NOE experiments for **4** were limited by its decreased solubility in $CDCl_3$ relative to **2** and **3** and suffered crucially from exchange between the lactam and the acid/residual H_2O protons within the relaxation time scale, resulting in saturation transfer. Therefore, it was not possible to confirm or exclude hydrogen bonding between the acid proton and the lactam oxygen. Based on the measured NOEs from the lactam proton to the acid carbon, it was also not possible to reach any firm conclusions about hydrogen bonding between the lactam NH and the acid carbonyl oxygen because irradiation of the lactam proton is expected to yield an NOE due to the saturation transfer to the acid proton. An intensity increase has been detected at the acid carbon when irradiating the pyrrole NH signal and is approximately in the range of the NOEs found for **2** and **3**. However, it cannot be ascertained whether it is a real NOE or an artifact because the overall experimental performance was very poor. Therefore, no firm conclusions could be reached.

(n=2) 10,10-Dimethylglaucorubin (5). $^1H\{^1H\}$-Homonuclear NOEs intensities are approximately the same as those found in **2** (Table 2). The only major difference is the higher value of the NOE that the acid OH protons receive from the lactam protons. This may be due to the much higher solubility of **5** compared to **2**, which allowed us to run the NOE experiments at higher concentrations of **5** where the relative amount of (unavoidable) traces of water is lower. This means that a larger percentage of the exchanging CO_2H and H_2O protons is relaxed in the acid site and thus these protons are more sensitive to population disturbances at the lactam protons. The values of the $^{13}C\{^1H\}$-heteronuclear NOEs of **5** are also very close to those determined for **2**, and significant NOEs from the lactam as well as from the pyrrole protons have been detected. In solution, therefore, **5** appears to have essentially the same conformation as **2**, and the methyl groups at C(10) in **5** do not impose any significant distortion of the ridge-tile solution structure.

Analyses of NOE Results in $(CD_3)_2SO$ Solvent. In pure $(CD_3)_2SO$ most $^1H\{^1H\}$-NOEs of **2** at 500 MHz are negative (Table 2). This may be attributed to the high viscosity of $(CD_3)_2SO$ compared to $CDCl_3$, yielding much longer correlation times and therefore shifting NOEs into the negative NOE region. (In accordance with expectations from theory,[21] we measured NOEs closer to zero at 300 MHz.) But the correlation times are still sufficiently small to keep the NOEs reasonably far away from spreading the saturation of a spin over the whole molecule; so, some qualitative conclusions are still possible. In contrast, quantitative or even semiquantitative interpretations are no longer possible, especially because under these circumstances the assumption of identical correlation times within the molecule no longer obtains. For theoretical reasons, $^{13}C\{^1H\}$-NOEs never become negative but only decrease. In $(CD_3)_2SO$, the total NOE that the acid carbon receives has dropped to about half the value in $CDCl_3$, and the NOE from the acid proton is diminished in the same order of magnitude. Only very small intensity changes of the acid carbon peak intensity have been detected when irradiating the lactam or the pyrrole protons. Overall, our experiments in $(CD_3)_2SO$ do not give any hint as to hydrogen bonding in this solvent, but due to the unfavorable properties of $(CD_3)_2SO$ for NOE studies, they should not be used to draw further inferences. These findings correct the erroneously high NOE values for **2** in $(CD_3)_2SO$ reported earlier from our laboratory.[15]

Analysis of NOE Results in $(CD_3)_2SO$-$CDCl_3$ Mixed Solvents. Because **2** shows intramolecular hydrogen bonding in pure $CDCl_3$ and does not give clear NMR evidence for hydrogen bonding in $(CD_3)_2SO$, we ran additional experiments in $(CD_3)_2SO$-$CDCl_3$ solvent mixtures in order to determine the volume % $(CD_3)_2SO$ necessary to drop the NOE to approximately zero.

$(CD_3)_2SO$-$CDCl_3$. A 10:90 by volume mixture of $(CD_3)_2SO$ and $CDCl_3$ already contains a large (1000x) molar excess of $(CD_3)_2SO$ compared to the concentration of the dissolved mesobilirubin. In this solvent mixture, large $^1H\{^1H\}$ NOEs between the lactam and the pyrrole protons are still present (Tables 2 and 3), indicating a *syn-Z* geometry between these ring. However, we were not able to detect NOEs between the lactam and the acid protons. There are two possible explanations for this fact. One possibility is that hydrogen bonding between the acid proton and the lactam oxygen is lost. The other possibility is that there is a cancellation of the effects of a positive NOE on one hand and a slight amount of saturation transfer (which is proven to take place for higher $(CD_3)_2SO$ percentages) on the other hand. In contrast, $^{13}C\{^1H\}$-NOE experiments in $(CD_3)_2SO$-$CDCl_3$ (10:90) still reveal significant NOEs from the lactam and the pyrrole protons to the acid carbon, providing a strong indication of a hydrogen-bonded conformation in **2** — even in the presence of a large molar excess of $(CD_3)_2SO$. Although it could not be clearly evaluated whether the hydrogen bond between the acid hydrogen and the lactam oxygen still exists, overall, these findings do not support the idea of a specific hydrogen bond breaking interaction between $(CD_3)_2SO$ and **2**.

In a 20:80 by volume mixture of $(CD_3)_2SO$ and $CDCl_3$, the values for the homonuclear NOEs between the lactam and the pyrrole protons dropped somewhat (Tables 2 and 3). In addition, under these conditions a small but significant saturation transfer between the acid/H_2O and the lactam protons is observed, indicating exchange between these protons. Given the uncertainties introduced by saturation transfer, conclusions concerning hydrogen bonding can no longer be drawn from the $^1H\{^1H\}$-NOEs.

In a 30:70 mixture of $(CD_3)_2SO$ and $CDCl_3$ the overall situation is about the same as in a 20:80 mixture. The NOEs between the lactam and the pyrrole protons have dropped further. Again, significant saturation transfer between the acid and the lactam protons is observed, indicating exchange between these protons.

The $^{13}C\{^1H\}$-NOE experiments in $CDCl_3$-$(CD_3)_2SO$ solvent mixtures containing ≥20% by volume

$(CD_3)_2SO$ suffer from the broad shape of the acid carbon peak, leading to a very poor signal to noise ratio. Limited pigment solubility limits our ability to overcome these problems simply by increasing its concentration. Additional problems arise from the saturation transfer between the acid/H_2O and the lactam protons, which exclude the detection of hydrogen bonding from any possible enhancements coming from the lactam proton to the acid carbon. Experimental performance was too poor to get any reliable values from the pyrrole proton. Overall we were not able to obtain reliable information on the question of intramolecular hydrogen bonding.

Analysis of NOE Results from $(CD_3)_2SO$-$(CD_3)_2CO$ Mixed Solvent. With respect to the unfavorable NOE properties of $(CD_3)_2SO$ we decided to run experiments in a 33:67 mixture (by volume) of $(CD_3)_2SO$-$(CD_3)_2CO$. The properties of both solvent are comparable so this mixture should be reasonable model for pure $(CD_3)_2SO$. The viscosity of such a mixture is much lower than the one of pure $(CD_3)_2SO$ and therefore should enable us to shift NOEs back into positive NOE region. $^1H\{^1H\}$-NOE experiments in this solvent mixture show that this approach is suitable, and the NOEs are now back in the positive NOE region (Tables 2 and 3). The NOEs between the lactam and the pyrrole protons are lower than the values in $CDCl_3$, especially when compared with the NOEs between the pyrrole and the bridging CH_2 protons. NOEs between lactam and pyrrole protons also do not significantly increase when running the experiments at lower field. These findings suggest a possible deviation from a pure *syn-Z* geometry between the lactam and the pyrrole rings in this solvent system. A small negative enhancement from the acid to the lactam protons indicates some saturation transfer due to exchange. In contrast, reverse transfer has not been seen, but this failure might be due to the intrinsically low sensitivity of acid proton enhancement detection because of the broad shape of this peak. Overall, the homonuclear NOE studies do not provide evidence for intramolecular hydrogen bonding in this solvent mixture.

In addition to NOEs from the acid and the side chain protons found in our $^{13}C\{^1H\}$-NOE experiments, we noted a small intensity change when saturating the lactam proton. However, this value is fundamentally lower than the corresponding value in $CDCl_3$, and close to the experimental error. (If it is actually considered significant, it is most likely caused by the weak saturation transfer between the lactam and acid protons that we detected in our $^1H\{^1H\}$-NOE studies. Irradiation of the lactam proton therefore also gives a small saturation of the acid proton, leading to a small acid carbon enhancement. However, such an enhancement is not caused by a spatial proximity of the lactam protons and the acid carbon.) No NOE from the pyrrole protons could be detected. Therefore, for **2** in $(CD_3)_2SO$-$(CD_3)_2CO$ we can exclude a pattern of intramolecular hydrogen bonding comparable to the hydrogen bonding that takes place when **2** is dissolved in $CDCl_3$.

Heteronuclear Distance Calculations. Within the two-spin approximation it is possible to determine internuclear distances (r_x) directly from the NOE values by using the equation[21,22]

$$NOE_x/NOE_{ref} = r_x^{-6}/r_{ref}^{-6} \quad (1)$$

if a reference distance (r_{ref}) is known. For the rubins investigated it is not possible to use this equation directly because significant indirect three-spin NOEs have to be taken into account. For evaluating carboxyl carbon to proton distances using heteronuclear NOEs from the carboxyl carbon, the molecule may be divided into two groups of protons (both appearing twice in the molecule) which can be treated virtually independently from the NOE point of view. The first group is formed by spins of the acid side-chains; whereas, the other group is formed by the spins of the (presumed) hydrogen bond array, namely the acid, the lactam and the pyrrole proton. All other protons may be neglected in this context because they do not give any significant NOEs to

the carboxyl carbon. Because within each of these groups irradiation of one proton substantially influences not only the spin populations of the acid carbon but also other protons within the group, indirect effects must be considered within each of these groups.

The NOE network and pathways for the presumed hydrogen bond array are shown in Fig. 2. One of the indirect pathways goes, *e.g.*, from the lactam proton *via* the acid proton to the acid carbon: Saturation of the lactam proton causes a positive NOE of the proton acid (*cf.* Table 2, $^{1}H\{^{1}H\}$-NOEs). The acid carbon peak intensity is strongly influenced by population disturbances at the acid proton (*cf.* Table 2, $^{13}C\{^{1}H\}$-NOEs). The population disturbance/intensity increase of the acid proton consequently causes an intensity decrease at the acid carbon. Overall this negative three-spin NOE contribution therefore diminishes the actual measured NOE from the lactam proton to the acid carbon (*cf.* Fig. 2C). This pathway is a very important indirect NOE pathway because the carboxyl carbon receives a very strong NOE from the carboxylic acid proton. Similar indirect pathways go from the lactam proton *via* the pyrrole proton to the carboxylic acid carbon, and from the pyrrole proton *via* the lactam proton to the carboxylic acid carbon, *e.g.* (*cf.* Fig. 2B, 2C).

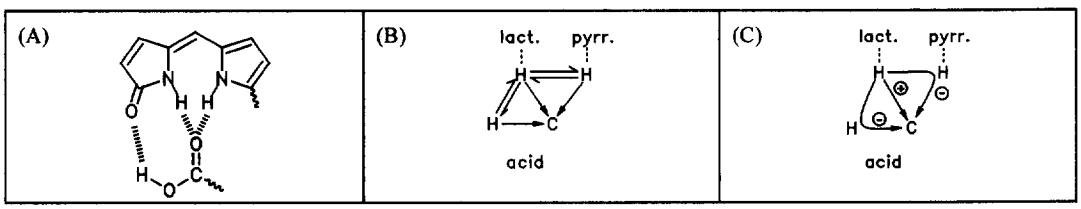

FIGURE 2. (A) Carboxylic acid to dipyrrinone hydrogen bonding in bilirubin analogs. (B) NOE pathways from the lactam and pyrrole NHs to the carboxyl carbon. (C) Direct ⊕ and indirect ⊖ NOE contributions from the lactam-NH to carboxylic acid carbon.

Since the acid proton is hydrogen bonded to the lactam oxygen, the bond length of the acid OH to lactam oxygen hydrogen bond and the O−H···O angle may be affected by the hydrogen bonding, as might the nonbonded distance between the acid OH and the acid carbon. Rather than taking the acid proton-acid carbon distance as the reference for the distance calculations, we chose the distance between an α-proton and the acid carbon distance. This distance should be independent of any conformational changes influenced by hydrogen bonding. The related NOEs from the side chain protons have not been measured (*vide supra*), but the expected direct NOE from these protons can be calculated using nonbonded distances obtained from the X-ray structure of bilirubin or from molecular modeling geometries. We derived the latter from molecular dynamics calculations using SYBYL. Because there are no significant NOE contributions other than from the hydrogen bond array and the acid side chain, the total NOE to the acid carbon minus the sum of direct NOEs from the protons of the hydrogen bond array yields the sum NOE from the acid side chain. This value was distributed between the side chain protons according to the side chain geometry to give the direct NOE from each of the α-protons. Based on these values we were then able to calculate proton to carboxylic acid carbon distances (Table 4) by using eq. (1).

To be able to calculate distances from these measured NOEs, we evaluated the direct NOE contributions to the carboxylic acid carbon coming from each of the protons in the hydrogen bonded array. This was accomplished using an iterative initial guess-best fit approach until a reasonable self-consistency of the detected NOE values was achieved within the limits of experimental error. For example, for **2** in $CHCl_3$ our initial guess for the direct NOE contributions to the acid carbon was 34.0% from the acid proton, 5.0% from the lactam proton, and 3.0% from the pyrrole proton. Together with the experimental $^{1}H\{^{1}H\}$-NOEs shown in Table 2

TABLE 4. Selected Nonbonded Distances (Å) in Mesobilirubin Carboxylic Acid-Dipyrrinone Hydrogen Bonded Partners, as Determined from Heteronuclear $^{13}C\{^1H\}$NOEs from the Lactam and Pyrrole NHs to the Acid Carbon at 25°C. Data Include: Experimental NOEs, Calculated Direct NOEs, Calculated Absolute Proton to Carbon Distances from NOEs and Distances Relative to the Acid Proton Distance. Distance Values are Based on an α-Proton Distance of 2.10Å to the Carboxyl Carbon, and on a Relative NOE Contribution from the Side Chain of 0.445 for Each of the α-Protons.

Pigment	Solvent	Lactam N-H				Pyrrole N-H				Acid Carbon			
		NOE (exptl)	NOE (direct)	Calc. Dist.[a]	Rel. Dist.	NOE (exptl)	NOE (direct)	Calc. Dist.[a]	Rel. Dist	NOE (exptl)	NOE (direct)	Calc. Dist.[a]	Rel. Dist.
1	$CDCl_3$	[b]				[b]				~35		~2.09 - 2.12[b]	1
2[d]	$CDCl_3$	3.5	6.0	2.80	1.42	2.5	3.6	3.05	1.55	49.3	49.5	1.97	1
2	$CDCl_3$	3.6	4.95	2.68	1.38	1.8	2.65	2.97	1.53	34.0	34.1	1.94	1
2	$CDCl_3$[e]	3.2	4.5	2.68	1.36	2.0	2.5	2.96	1.50	28.7		1.97	1
2	$CDCl_3$[f]	4.0		~2.7[g]	1.36	2.2		~3.0[g]	1.52	33.0		1.98	1
2	$CDCl_3$ 90% $(CD_3)_2SO$ 10%	3.1	3.45	2.79	1.45	1.7	2.2	3.01	1.57	32.4		1.92	1
2	$CDCl_3$ 80% $(CD_3)_2SO$ 20%	[h]								25.8		2.06-2.11[c]	1
2	$CDCl_3$ 70% $(CD_3)_2SO$ 30%	[h]								25.7		1.98-2.03[c]	1
2	$(CD_3)_2CO$ 67% $(CD_3)_2SO$ 33%	0.7[h]	0.7	>3.85[i]	>1.78	0.1	0.1	5.33[i]	2.45	22.2		2.16	1
2	$(CD_3)_2SO$	0.3	0.3	4.02[i]	1.92	0.2	0.2	4.30[i]	2.06	14.4		2.09	1
3	$CDCl_3$	4.3	4.73	2.51	1.38	2.3	3.15	2.68	1.48	38.6		1.81	1
4	$CDCl_3$	[h]				[b]				32.4		1.95-1.99[c]	1
5	$CDCl_3$	3.6	6.48	2.57	1.32	1.8	2.65	2.98	1.53	34.0	34.2	1.95	1
5	$CDCl_3$[j]	3.2	5.32	2.67	1.36	1.5	2.11	3.12	1.59	34.6	34.8	1.96	1
BR-IXα	X-Ray Structure			2.66[k]				2.91[k]				2.07[k]	
2	SYBYL			2.46[l]				2.79[l]				1.89[l]	
3	SYBYL			2.80[l]				2.85[l]				1.92[l]	
5	SYBYL			2.72[l]				2.94[l]				1.91[l]	

[a] Distance in Å, ±5%. [b] Reliable experimental values unavailable. [c] Estimated values: higher value, non-hydrogen bonded form; lower value, estimate for a hydrogen bonded form (determined based on the usual NOE values). [d] Run on a GN-300 MHz GE NMR. [e] 0°C. [f] 37°C. [g] Estimated value based on contributions of indirect effects at 25°C. [h] Saturation transfer. [i] ±1 Å. [j] 10 mm broad band probe at 500 MHz. [k] Using data from ref. 6. [l] Molecular dynamics on an E&S Workstation using SYBYL (ref. 8).

(line 2), one would then expect an experimental heteronuclear NOE to the acid carbon of 3.586% (*i.e.*, 5.0% diminished by 3.0 x 0.222% *via* the pyrrole proton and diminished by 34.0 x 0.022% *via* the acid proton) when irradiating the lactam proton. When irradiating the pyrrole proton we would expect an NOE of 2.137% at the acid carbon (*i.e.*, 3.0% diminished by 5.0 x 0.203% *via* the lactam proton plus a positive four-spin contribution of 34.0 x 0.022 x 0.203% *via* the lactam and the acid proton). Because the experimental value from the pyrrole proton is only 1.8% and not 2.137%, our initial guess for this proton was too high. Therefore, we repeated the entire procedure with an improved direct contribution value, and after few iterations we were able to achieve a satisfactory consistency with the experimental values. The results for the direct NOE contribu-

tions, now directly related to the internuclear distances, are shown in Table 4. (For completeness, and to give approximate values, the experimental values for **2** in $(CD_3)_2SO$-$(CD_3)_2CO$ and in pure $(CD_3)_2SO$ have been transformed into nonbonded distance in Table 4.)

Results from Distance Calculations and Interpretation. As indicated in Table 4, the lactam and pyrrole NH to carboxylic acid carbon distances of **2**, **3** and **5** fall well within those expected for hydrogen bonding in $CDCl_3$. The values determined for the carboxylic acid carbon to carboxyl hydrogen distances for **2** and **5** compounds vary from 1.92-1.98Å; the values for the lactam carbon distances vary from 2.57-2.80; and the values for the pyrrole carbon distances vary from 2.96-3.12Å. The lactam and pyrrole distances are in good agreement with the values from the X-ray crystal structure of bilirubin, but the X-ray structure shows a slightly longer distance between the acid OH and acid carbon. The latter fact may be due to packing forces in the solid state. The general agreement between the results from both methods provides additional confirmation that we used a correct experimental set-up for our NOE experiments. The relevant distances for **2** found in its energy-minimum structure determined using molecular dynamics (SYBYL)[8] are slightly lower than those from NOEs and those from X-ray crystallography. For homolog **3**, all distances were determined to be slightly shorter than in **2**, but the relative ratios of the distances are still about the same, consistent with the prevalence of a hydrogen-bonded ridge-tile conformation akin to that of Fig. 1.

Our studies in $(CD_3)_2SO$-$CDCl_3$ mixtures show that **2** is still intramolecularly hydrogen bonded in $CDCl_3$ containing 10% (vol) $(CD_3)_2SO$. There is uncertainty whether the acid proton to lactam oxygen hydrogen bond is still present. The small acid proton to acid carbon distance, which according to Table 4 seems to be an indicator for hydrogen bonding, would support such hydrogen bonding between the acid proton and lactam oxygen, but we have not been able to detect a $^1H\{^1H\}$-NOE between the lactam and acid proton. Compared to the distances determined in pure $CDCl_3$, the distance determined between the lactam NH and the carboxyl carbon is slightly higher. However, it may be concluded that even the presence of 10^3 mole equivalents of $(CD_3)_2SO$ cannot prevent intramolecular hydrogen bonding in **2**. For higher % $(CD_3)_2SO$, we were unable to obtain reliable NOE information, but the slightly longer acid carbon to acid OH non-bonded distances hint at a possibly less tightly hydrogen-bonded conformation. In contrast, in $(CD_3)_2CO$-$(CD_3)_2SO$ both the lactam proton and the pyrrole proton to acid carbon distances are determined to be much higher. Therefore, in this solvent system (and, as far as conclusions may be drawn, also in pure $(CD_3)_2SO$), **2** does not adopt the conventional (Fig. 1) intramolecularly hydrogen bonded form. This is also supported by a slightly, but significantly longer acid proton to acid carbon distance of 2.1 Å (vs ~1.95 Å in $CDCl_3$). The various non-bonded distances from the lactam NH and pyrrole NH to the carboxyl carbon determined in this work and earlier studies[6,7] are summarized in Table 5.

TABLE 5. Carboxyl Carbon to Dipyrrinone N-Hydrogen Distances in [8³,12³-C_2]-Mesobilirubin-XIIIα (**2**) as Measured by $^{13}C\{^1H\}$-NOE NMR Spectroscopy.

Distance From Carboxyl Carbon to	Di-Acid		
	Distance to $^{13}CO_2H$ Carbon (Å) in		
	$CDCl_3$[a]	$(CD_3)_2CO$-$(CD_3)_2SO$[b]	Crystal[c]
Lactam N-H	2.7	>3.9	2.7
Pyrrole N-H	3.0	~5.3	2.9

[a] ± 0.1 Å. [b] ± 1 Å. [c] References 6 and 7.

CONCLUDING COMMENTS

Our $^1H\{^1H\}$ and $^{13}C\{^1H\}$-NOE studies of **1-5** provide evidence for the existence of a hydrogen-bonded conformation in non-polar solvents for the compounds with propionic (**2** and **5**) and butanoic acid (**3**) side chains. The distances determined between the carboxyl carbon and the lactam and pyrrole NHs (Tables 4 and 5) are in good agreement with the values from the X-ray structure of bilirubin. Interestingly no major changes occur in mixed solvent systems which contain the non-polar solvent and significant amounts of a polar solvent ($(CD_3)_2SO$) known to interfere with hydrogen bonding. The very low solubility of pigments with an acetic acid side chain (**1**) and a pentanoic acid side chain (**4**) prevented us from obtaining good NOE data. For mesobilirubin esters (**7** and **8**), hydrogen bonding such as that found in Fig. 1 can be excluded. The exact solution conformation of these compounds is still unknown and is the focus of on-going investigations.

EXPERIMENTAL

General Procedures. High resolution nuclear magnetic resonance (NMR) spectra were determined in on a Varian Unity Plus 500 MHz spectrometer or a General Electric GN-300 300 MHz spectrometer and are reported in δ (ppm) downfield from $(CH_3)_4Si$. Infrared spectra were run on a Perkin Elmer 1610 FT-IR; ultraviolet-visible spectra were run on a Cary 219 spectrophotometer. High resolution mass spectra were performed by the Midwest Center for Mass Spectrometry with partial support by NSF, Biology Division (Grant No. DIR-9017762), Lincoln, NE. GC-MS analyses were carried out on a Hewlett-Packard GCMS Model 5890A ion selective detector equipped with a DB-1 (100% dimethylpolysiloxane) column. Melting points were determined on a Thomas-Hoover Uni-Melt capillary apparatus and are uncorrected. All solvents were reagent grade obtained from Fisher. Deuterated chloroform, acetone and dimethylsulfoxide were from Cambridge Isotope Laboratories. Labelled potassium cyanide ($K^{13}CN$, 90% and 99% ^{13}C-enriched) were obtained from Cambridge Isotope Laboratories. *p*-Chloranil was obtained from Eastman Kodak and used as received. $NaBH_4$ was from J.T. Baker and formic acid and $CaCl_2$ were from Fisher, all used as received. 2,2-Dimethoxypropane, trifluoroacetic acid and sulfuryl chloride were obtained from Aldrich. Analytical thin layer chromatography (TLC) was carried out on J.T. Baker silica gel IB-F plates (125 μm layer). Flash chromatography was performed on Woelm silica gel F, thin layer chromatography grade.

NMR Experiments. Nuclear magnetic resonance (NMR) T_1 and NOE measurements were performed on a Varian Unity 500 MHz NMR equipped with linear amplifiers on a 5 mm broadband probe. Due to the extremely poor solubility of rubins **1** and **4**, a 5 mm indirect probe was used for proton experiments and a 10 mm broadband probe for ^{13}C experiments. Some additional experiments were also performed on a General Electric GN 300 MHz NMR equipped with a 10 mm broadband probe. The solvent was used as internal reference (*e.g.*, $CDCl_3$: ^1H residual $CHCl_3$ = 7.26 ppm; ^{13}C = 77.0 ppm). All experiments were run at 25°C unless otherwise noted. Standard parameter values were: ^1H: frequency = 499.863 MHz, 90° pulse = 32 μs, acquisition time = 2.999 s, sweep width = 11022 Hz, filterband = ±6200 Hz, number of points = 66112, zero filled to 256K, line broadening = 0.2 Hz, 1 Hz for NOE difference experiments. ^{13}C: sfrq = 125.712 MHz, 90° pulse = 10.4 μs, acquisition time = 4.009 s, sweep width = 2514 Hz, filterband = ±1400 Hz, number of points = 20160, zero filled to 128K or 256K for the best peak definition, line broadening = 0.5 Hz. All ^{13}C experiments were run applying a WALTZ-16 decoupling scheme during acquisition.

Sample Preparation. $CDCl_3$ was dried by standing over P_2O_5 and subsequently filtered over Woelm basic Al_2O_3, Act. I. $(CD_3)_2SO$ and $(CD_3)_2CO$ were dried over 3Å molecular sieves. Nearly saturated solutions were prepared by treating an excess of rubin with the solvent, gently heating, then letting it stand for at least 30 min. To remove excess, non-dissolved rubin, samples were filtered into the NMR tube. No attempt was made to determine the actual amount of rubin in the NMR sample. Samples were not degassed, in order to maintain constant experimental conditions (O_2 concentration), and it has also turned out that relaxation due to O_2 did not significantly influence the NOE measurements. Despite our serious attempts to exclude water, our samples still contained significant amounts of water related to the amount of dissolved rubin, especially for those with very poor solubility. In all cases the acid protons and the H_2O protons were in fast exchange on the relaxation time scale, yielding in almost full saturation transfer when irradiating either.

NOE Measurements. To prepare for the NOE study, T_1 measurements of the ^{13}C-labelled CO_2H and CO_2CH_3 groups in bilirubin analogs **1-5** were carried out using the inversion recovery method and standard system macros for the experimental setup and calculations. (^1H: nonselective T_1, ^{13}C: selective T_1.) The ^{13}C chemical shift data and T_1 data are shown in Table 1. For the NOE experiments, the pulse sequence 'cycledof' using the decoupler channel for preirradiation contained in the user library was employed for both $^1H\{^1H\}$ and $^{13}C\{^1H\}$-NOE experiments. The pulse sequence source code had to be slightly modified in order to make the sequence run on our system, and an additional linear attentuator (saturation fine power, 'satpwrf') was included, but the fundamentals of the pulse sequence remained unchanged. Reference spectra were determined by setting the preirradiation frequency at large offset (−5000 Hz), and usually several reference spectra were taken in order to reduce errors (every 3 to 5 spectra). Experiments were run in an interleaved mode, usually cycling between irradiation targets every block size of 8 transients. Preirradiation times were at least 5 times the longest T_1 (Table 1) in the system (usually 20-30 s). Interpretation of the NOE values is based on the assumptions that variations of T_c within the molecule are negligible.

For the homonuclear and heteronuclear NOEs, we first obtained reproducible high resolution ^1H-NMR spectra with well-separated signals. The closest lying signals were from the pyrrole and lactam NHs, with 1.5-2 ppm separation, depending on solvent. For $^1H\{^1H\}$-NOE experiments, the saturation power ('satpwrf') was usually set to a value of 2, achieving approximately a 60-80% saturation of the irradiation target, depending on peak shape and T_1. NOEs were determined by integration of the NOE difference peaks, using the irradiation target (and considerating the numbers of protons) as the reference. Typical experiments were run with the number of transients (NT)=64 and from reproducibility errors are estimated to be better than 1/10 of the reported NOE value or ~0.5% absolute. For $^{13}C\{^1H\}$-NMR experiments, total NOEs were determined from full-time decoupled spectra in comparison to gated decoupled spectra. Selective NOE experiments were run with 100% saturation of the irradiation target. The saturation power ('satpwrf') was usually set to a value of −5, the additional linear attentuator ('satpwrf') was usually set to a value of 3072 (=75%). For pre-irradiation of the acid peak a somewhat higher power level had to be used. Note that in comparison to homonuclear experiments this value is lower (*cf.* below). Care was taken to ensure that on one hand the irradiation target was completely saturated, and on the other hand accidental saturation of neighbor peaks did not occur. We determined that for most measurements we irradiated the selected proton frequency at a width ± 50 Hz. Repeat NOEs at 50% lower saturation power gave the same but weaker NOEs of the observed carbon signals. Peak intensities were determined using peak fitting routines. In our hands this proved to be the most reliable method; it is superior to normal integration or area determinations from difference spectra. Typically, the number of transients varied between NT=64 and NT=256; the reported NOE values are usually an average of at least five runs. Errors are estimated from reproducibility to be better than ~1/20 of the reported NOE value, or ~0.5%

absolute. Errors in non-bonded distances calculated (eq. 1) from the NOEs are ±0.1 Å in most cases.

Cautionary Note and Saturation Power: In running and interpreting NOE experiments it is crucially important to know the exact extent of saturation of the irradiation target and to avoid any unwanted accidental saturation of neighboring peaks. This is not a problem, of course, when running homonuclear NOE experiments because the recorded spectra give you this information directly. It is a problem, however, when running heteronuclear NOEs. On the Varian 500 MHz instrument (and to our knowledge on most commercially available instruments), it is not possible to know the exact extent of saturation from running an otherwise identical experiment with detection of the preirradiated nucleus because the instrument uses a different signal routing for homo and for heteronuclear experiments. This means that for identical parameter settings (same number for the saturation power) much more power is actually going into the sample when running heteronuclear experiment than when running homonuclear experiments. We found the best approach to control and cope with this problem is to attempt a full saturation of the irradiation target when running heteronuclear NOE experiments. Well-separated proton signals for NH, OH and CH[8,13,16,18,20,25,26] were irradiated selectively. The correct saturation power can then be evaluated by investigating the NOE behavior of a heteronucleus when irradiating the target peaks with a number of different power values. With a correct power level the NOE should remain constant within a certain range of increasing power levels. On the other hand, the NOE should increase when the irradiation target has not yet been fully saturated (due to an increasing extent of saturation), and when accidental saturation of neighboring peaks is relevant (due to an increasing NOE contribution from those neighboring peaks).

Preparation of [C^2_8, C^2_{12} - ^{13}C]-Mesobilirubin-XIIIα (1). Using a standard set of transformations,[18] [C_8^2-^{13}C] nor-xanthobilirubic acid (**14**)[27] was converted to rubin **1** as follows:

(n=1) [C_8^2,C_{12}^2-$^{13}C_2$]-Mesobiliverdin-XIIIα Dimethyl Ester (10). In a 500 mL round bottom flask equipped with a magnetic stir bar and condenser was placed nor-xanthobilirubic acid methyl ester **14**[27] (500 mg, 1.65 mmol) in CH_2Cl_2 (375 mL). To this was added *p*-chloranil (1.60 g, 6.51 mmol) followed by 88% formic acid (40 mL). The reaction immediately turned green and was heated at reflux for 24 h. The emerald green solution was concentrated to ~75 mL then cooled to −20°C to precipitate the reduced *p*-chloranil, which was removed *via* filtration and washed with ice cold CH_2Cl_2. The filtrate was washed cautiously with 5% $NaHCO_3$ (3 x 100 mL), then dried over anhyd Na_2SO_4, filtered, and concentrated to dryness to afford a blue solid. The solid was dissolved in a minimum amount of CH_2Cl_2 and deposited on an aspirator suction filtration flash column (3 x 4.5 cm diameter) loaded with silica gel, pre-eluted with CH_2Cl_2, and eluted with CH_2Cl_2-CH_3OH (10:1) to remove a dark blue band, which was collected and concentrated to dryness then to afford verdin ester **10** as a blue solid (402 mg, 0.683 mmol, 83%). It had mp 201-203°C (Lit.[18] 202-203°C); ^{1}H-NMR ($CDCl_3$) δ: 1.21 (t, 6H, 2 x CH_2CH_3, $^3J_{HH}$=7.5 Hz), 1.81 (s, 6H, C_7/C_{13} CH_3), 2.11 (s, 6H, C_2/C_{18} CH_3), 2.49 (q, 4H, 2 x CH_2CH_3, $^3J_{HH}$=7.5 Hz), 3.58 (d, 4H, $CH_2{}^{13}CO_2CH_3$, $^2J_{CH}$=7.9 Hz), 3.70 (d, 6H, 2 x OCH_3, $^3J_{CH}$=3.8 Hz), 5.92 (s, 2H, C_5/C_{15} 2 x CH), 6.76 (s, 1H, C_{10} CH), 8.25 (brs, 3H, NH pyrrole and 2 x NH lactam) ppm; ^{13}C-NMR ($CDCl_3$) δ: 170.91 (C_8^2/C_{12}^2 C=O) ppm (8 scans). The material was used directly in the next step.

(n=1) [C_8^2,C_{12}^2-$^{13}C_2$]-Mesobilirubin-XIIIα Dimethyl Ester (6). In a 125 mL Erlenmeyer flask was placed verdin ester **10** (202 mg, 0.343 mmol) in N_2-saturated CH_3OH (30 mL). This was then placed in a sonicator, where $NaBH_4$ (1.00 g, 26.4 mmol) was added; and the mixture was swept with N_2 and sonicated for 30 min. The resulting yellow suspension was cooled to 4°C, acidified to pH 8 by addition of 10% HCl and extracted with CH_2Cl_2 (200 mL). The extract was washed with water (2 x 200 mL) and saturated aq NaCl

(1 x 200 mL), dried over anhyd Na_2SO_4, filtered, and concentrated to dryness to afford the yellow-green solid rubin ester. The crude rubin ester was then dissolved in a minimum amount of CH_2Cl_2 and deposited on a silica gel aspirator flash column (2.5 x 4.5 cm diameter), pre-eluted with CH_2Cl_2 and eluted with CH_2Cl_2:ethanol (100:1) to remove a yellow band which was collected and concentrated to dryness to afford the rubin as a yellow solid (120 mg, 0.204 mmol, 59%). It had mp 253-255°C (Lit.[18] 254-256°C); ^{1}H-NMR ($CDCl_3$) δ: 1.12 (t, 6H, 2 x CH_2CH_3, ^3J=7.5 Hz), 1.86 (s, 6H, C_7/C_{13} CH_3), 2.10 (s, 6H, C_2/C_{18} CH_3), 2.50 (q, 4H, 2 x CH_2CH_3, $^3J_{HH}$=7.6 Hz), 3.60 (d, 4H, $CH_2{}^{13}CO_2CH_3$, $^2J_{CH}$=7.6 Hz), 3.92 (s, 2H, C_{10} CH_2), 4.02 (d, 6H, 2 x OCH_3, $^3J_{CH}$=3.8 Hz), 5.90 (s, 2H, C_5/C_{15} CH), 8.53 (brs, 2H, 2 x NH pyrrole), 10.15 (brs, 2H, 2 x NH lactam) ppm; ^{13}C-NMR ($CDCl_3$) δ: 175.95 ($C_8{}^2/C_{12}{}^2$ C=O ppm (8 scans). The material was taken directly to the next step.

(n=1) [$C_8{}^2$,$C_{12}{}^2$-$^{13}C_2$]-Mesobilirubin-XIIIα (1). In a 25 mL round bottom flask equipped with a magnetic stir bar and reflux condenser was placed rubin ester **6** (40.0 mg, 0.068 mmol) in THF (10 mL), CH_3OH (5 mL), and 1 M NaOH (1.5 mL). The mixture was heated to reflux for 3 h; then, orange suspension was cooled in an ice bath and acidified with 1 M HCl (6 mL). The resulting yellow-green suspension was extracted with CH_2Cl_2, which was washed with water, saturated aq NaCl, and concentrated to dryness to afford a yellow green solid. The crude rubin was then suspended in CH_2Cl_2:CH_3OH (10:1) and cooled to −10°C. The solid collected by filtration and washed with CH_3OH, cooled to −10°C, filtered and dried to afford the rubin as a yellow solid (84.1 mg, 0.149 mmol, 73%). It had mp 205-207°C (Lit.[18] 205-207°C); ^{1}H-NMR 500 MHz ($(CD_3)_2SO$) δ: 1.08 (t, 6H, 2 x CH_2CH_3, $^3J_{HH}$=7.1 Hz), 1.77 (s, 6H, C_7/C_{13} CH_3), 1.96 (s, 6H, C_2/C_{18} CH_3), 2.49 (q, 4H, 2 x CH_2CH_3, under $(CD_3)_2SO$ peak), 3.09 (d, 4H, $CH_2{}^{13}CO_2H$, $^2J_{CH}$=6.7 Hz), 3.95 (s, 2H, C_{10} CH_2), 5.95 (s, 2H, C_5/C_{15} CH), 9.80 (brs, 2H, 2 x NH pyrrole), 10.35 (brs, 2H, 2 x NH lactam) 12.02 (brs, 2H, 2 x $^{13}CO_2H$) ppm; ^{13}C-NMR ($(CD_3)_2SO$) δ: 8.11 ($C_3/C_{17}{}^2$ CH_3), 9.36 ($C_7{}^1/C_{13}{}^1$ CH_3), 14.87 ($C_2{}^1/C_{18}{}^1$ CH_3), 17.17 ($C_3{}^1/C_{17}{}^1$ CH_2), 23.44 (C_{10} CH_2), 29.33 (d, $C_8{}^1/C_{12}{}^1$ CH_3, $^1J_{CC}$=55 Hz), 97.59 (C_5/C_{15} CH), 114.36 (d, C_8/C_{12}, $^3J_{CC}$=1.9 Hz), 122.16 (C_7/C_{13}), 123.10 (C_6/C_{14}), 123.17 (C_2/C_{18}), 128.15 (C_4/C_{16}), 130.76 (C_9/C_{11}), 147.25 (C_3/C_{17}), 171.99 (C_1/C_{19} C=O), 173.03 (d, $C_8{}^2/C_{12}{}^2$ C=O, $^1J_{CC}$=55 Hz) ppm; HR-MS *m/z* calcd. for $^{13}C_2C_{29}H_{36}N_4O_6$, 562.2702; found, 562.2703.

Preparation of (n=2) [8^3,12^3-$^{13}C_2$]-Mesobilirubin-XIIIα (2). This rubin was prepared from methyl [8^3-^{13}C]-xanthobilirubinate (**15**)[23,24,30] as reported previously[30] using the procedure outlined in the Synthetic Scheme.

Preparation of (n=3) [8^4,12^4-C_2]-Mesobilirubin-XIIIα (3). This rubin was prepared as outlined below using the procedures partly developed in the synthesis of **2**:[18,23,24,30]

3,5-Dimethyl-2-(ethoxycarbonyl)-1H-pyrrole-3-propanoic Acid (28). As described for the synthesis of **27**,[30] propionic acid analog, **28** was prepared from **32** in 88% yield and used directly in the next step. It had mp 153-154°C; ^{1}H-NMR, δ: 1.35 (3H, t, J=7.1 Hz), 2.16 (3H, s), 2.27 (3H, s), 2.48 (2H, t, J=7.6 Hz), 2.73 (2H, t, J=7.5 Hz), 4.30 (2H, q, J=7.1 Hz), 9.2 (1H, brs), 10.0 (1H, brs) ppm; ^{13}C-NMR, δ: 10.63 (q), 11.27 (q), 14.52 (q), 19.53 (t), 34.94 (t), 59.95 (t), 116.9 (s), 119.6 (s), 127.1 (s), 130.7 (s), 162.4 (s), 178.5 (s) ppm; GC-MS (EI), *m/z*: 239 (30%) [$M^{+\bullet}$], 194 (20%) [M - OC_2H_5 or M - CO_2H], 180 (80%) [M - CH_2CO_2H], 134 (100%) amu.

Ethyl 3,5-Dimethyl-4-(3-hydroxypropyl)-1H-pyrrole-2-carboxylate (25). As described previously for the synthesis of **24**,[30] its hydroxypropyl analog **25** was prepared from **28** in 99% yield and used directly in the next step. It had mp 107-107.5°C; ^{1}H-NMR, δ: 1.34 (3H, t, J=7.1 Hz), 1.70 (2H, m), 2.05 (1H, s), 2.20 (3H, s), 2.27 (3H, s), 2.45 (2H, t, J=7.5 Hz), 3.62 (2H, t, J=6.4 Hz), 4.29 (2H, q, J=7.1 Hz), 8.8 (1H, brs)

ppm; ^{13}C-NMR, δ: 10.57 (q), 11.40 (q), 14.54 (q), 20.14 (t), 33.42 (t), 59.61 (t), 62.33 (t), 116.8 (s), 121.2 (s), 127.0 (s), 129.7 (s), 161.8 (s) ppm; GC-MS (EI) *m/z*: 225 (30%) [$M^{+\bullet}$], 180 (80%) [M − OC_2H_5 or M − CH_2CH_2OH], 134 (100%) amu.

Ethyl 3,5-Dimethyl-4-(3-tosyloxypropyl)-1H-pyrrole-2-carboxylate (22). As described previously for the 3-tosyloxypropyl analog,[30] **22** was prepared from **24** in 83% yield and used directly in the next step. It had mp 102-103°C; ^{1}H-NMR ($CDCl_3$) δ: 1.34 (3H, t, J=7.1 Hz), 1.75 (2H, m), 2.14 (3H, s), 2.16 (3H, s), 2.38 (2H, t, J=7.5 Hz), 2.44 (3H, s), 3.98 (2H, t, J=6.2 Hz), 4.28 (2H, q, J=7.1 Hz), 7.78/7.33 (4H, AX, J=8.3 Hz), 8.8 (1H, brs) ppm; ^{13}C-NMR ($CDCl_3$) δ: 10.50 (q), 11.35 (q), 14.54 (q), 19.71 (t), 21.59 (q), 29.62 (t), 59.64 (t), 69.81 (t), 117.0 (s), 119.8 (s), 126.8 (s), 127.8 (d), 129.8 (d), 130.2 (s), 133.1 (s), 144.7 (s), 161.6 (s) ppm.

Ethyl 3,5-Dimethyl-4-(3-^{13}CN-cyanopropyl)-1H-pyrrole-2-carboxylate (19). As described for **18**,[30] the 3-tosyloxypropyl analog was prepared from **22** in 84% yield and used directly in the next step. It had mp 106-106.5°C; FT-IR (KBr) ν: 3286, 2985, 2921, 2194 (^{13}C≡N), 1661, 1446, 1269, 1172, 1097, 1022 cm^{-1}; ^{1}H-NMR ($CDCl_3$) δ: 1.35 (3H, t, J=7.2 Hz), 1.79 (2H, m), 2.22 (3H, s), 2.26 (3H, s), 2.31 (2H, m), 2.53 (2H, t, J=7.4 Hz), 4.30 (2H, q, J=7.2 Hz), 8.8 (1H, brs) ppm; ^{13}C-NMR ($CDCl_3$) δ: 11.02 (q), 11.87 (q), 14.96 (q), 17.07/16.33 (dt, $^1J_{CC}$=56 Hz), 23.19 (t), 26.64 (t), 60.13 (t), 117.6 (s), 119.7 (s), 120.2 ("s"), 127.2 (s), 130.3 (s), 162.1 (s) ppm; GC-MS (EI), *m/z*: 235 (30%) [$M^{+\bullet}$], 206 (10%) [M-C_2H_5], 190 (20%) [M - OC_2H_5], 180 (80%) [M - $CH_2CH_2{}^{13}C{\equiv}N$], 134 (100%) amu.

Methyl [8^4-^{13}C]-2,7,9-Trimethyl-3-ethyl-(10H)-dipyrrinone-8-butanoate (16). As described for the synthesis of the (n=2) xanthobilirubinate methyl ester (**15**),[27] ^{13}C-labelled nitrile **20** was converted to its diacid after saponification by heating in base for 36 hours, and the diacid was converted directly to the methyl (n=3)-xanthobilirubinate (**16**) in 63% yield. It had mp 185-187°C [lit.[31], mp 185-187°C]; UV-vis ($CHCl_3$): ε_{408}^{max} 31,400; FT-IR (KBr) ν: 3357, 2965, 2932, 2856, 1686, 1676, 1635, 1448, 1421, 1366, 1269, 1173, 1145 cm^{-1}; ^{1}H-NMR ($CDCl_3$) δ: 1.17 (3H, t, J=7.8 Hz), 1.78 (2H, m), 1.95 (3H, s), 2.12 (3H, s), 2.32 (2H, dt, $^3J_{HH}$=8 Hz, $^2J_{CH}$= 7.5 Hz), 2.39 (3H, s), 2.43 (2H, t, J=8 Hz), 2.55 (2H, q, J=7.8 Hz), 3.66 (3H, d, $^3J_{CH}$=3.8 Hz), 6.15 (1H, s), 10.3 (1H, brs), 11.3 (1H, brs) ppm; ^{13}C-NMR ($CDCl_3$) δ: 8.52 (q), 9.63 (q), 11.62 (q), 15.05 (q), 17.96 (t), 23.49 ("t"), 25.81 (t), 33.77/33.00 (dt, $^1J_{CC}$=58 Hz), 51.46 ("q"), 101.1 (d), 119.9 (s), 2 x 122.4 (s), 124.8 (s), 127.1 (s), 131.6 (s), 148.3 (s), 174.1 (s), 174.2 ("s") ppm. It was used directly in the next step.

(n=3) [8^4,12^4-$^{13}C_2$]-Mesobiliverdin-XIIIα Dimethyl Ester (12). As reported for the synthesis of (n=2) verdin ester **11** analog,[30] dipyrrinone **16** was oxidatively coupled to give the (n=3) verdin dimethyl ester (**11**) in 90% yield after flash chromatography. It had mp 180-182°C [lit.[18] mp 179-183°C]; UV-vis: ε_{369}^{max} 47,900, ε_{640}^{max} 14,300 ($CHCl_3$); FT-IR (KBr) ν: 3422, 3225, 2966, 2931, 2861, 1690, 1590, 1461, 1390, 1232, 1098 cm^{-1}; ^{1}H-NMR ($CDCl_3$) δ: 1.22 (6H, t, J=7.5 Hz), 1.83 (6H, s), 1.87 (4H, m), 2.07 (6H, s), 2.39 (4H, 'q'), 2.50 (4H, q, J=7.5 Hz), 2.64 (4H, t, J=7.5 Hz), 3.68 (6H, 'd', $^3J_{CH}$=3.7 Hz), 5.93 (2H, s), 6.78 (1H, s), 8.2 (3H, brs) ppm; ^{13}C-NMR ($CDCl_3$) δ: 8.36 (q), 9.53 (q), 14.47 (q), 17.85 (t), 23.56 ('t'), 26.30 (t), 33.49/32.72 (dt, $^1J_{CC}$=57 Hz), 51.53 ('q'), 96.29 (d), 114.2 (d), 127.8 (s), 128.3 (s), 138.7 (s), 139.8 (s), 141.4 (s), 146.7 (s), 149.9 (s), 172.5 (s), 173.9 (s) ppm. It was used directly in the next step.

(n=3) [8^4,12^4-$^{13}C_2$]-Mesobilirubin-XIIIα Dimethyl Ester (8). The corresponding (n=3) verdin (**12**) was reduced with sodium borohydride in 90% yield, as described previously for the (n=2) verdin.[24] It had mp 218-220°C [lit.[18] mp 219-221°C]; UV-vis: ε_{381}^{max} 54,000, ε_{420}^{sh} 29,000 ($CHCl_3$); FT-IR (KBr) ν: 3348, 2968, 2926, 1676, 1655, 1630, 1456, 1363, 1171, 980 cm^{-1}; ^{1}H-NMR ($CDCl_3$) δ: 1.00 (6H, t, J=7.8 Hz), 1.48 (6H, s), 1.81 (4H, m), 2.09 (6H, s), 2.34 (8H, m), 2.57 (4H, t, J=7.5 Hz), 3.67 (6H, d, $^3J_{CH}$=3.8 Hz), 4.09 (2H, s), 5.92 (2H, s), 10.3 (2H, brs), 10.6 (2H, brs) ppm; ^{13}C-NMR ($CDCl_3$) δ: 7.85 (q), 9.74 (q), 14.76 (q), 17.79 (t), 22.68 (t), 23.90 (t), 26.27 (t), 33.81/33.05 (dt, $^1J_{CC}$=57 Hz), 51.47 ('q'), 100.2 (d), 119.4 (s), 122.8 (s), 123.5 (s), 123.8 (s), 128.9 (s), 131.0 (s), 146.9 (s), 173.9 (s), 174.3 (s) ppm. It was used directly in the next step.

(n=3) [8⁴,12⁴-$^{13}C_2$]-Mesobilirubin-XIIIα (3). As described previously for the synthesis of rubin **2**,[18,24] the (n=3) rubin dimethyl ester (**8**) was saponified to give **3** in 88% yield after recrystallization. It had mp 279-281°C [lit.[18] mp 280-282°C]; UV-vis: ε_{429}^{max} 44,300, ε_{397}^{max} 37,200 ($(CH_3)_2SO$); FT-IR (KBr) ν: 3414, 2967, 2924, 2854, 1664, 1655, 1638, 1400, 1144 cm^{-1}; ^{1}H-NMR ($(CD_3)_2SO$) δ: 1.07 (4H, t, J=7.6 Hz), 1.35 (4H, m), 1.77 (6H, s), 1.98 (6H, s), 2.06 (4H, 'q'), 2.19 (dt, $^3J_{HH}$=7.5 Hz, $^3J_{HC}$=7.7 Hz), 2.49 (4H, 'q'), 3.94 (2H, s), 5.93 (2H, s), 9.9 (2H, brs), 10.7 (2H, brs), 11.9 (2H, brs) ppm; ^{13}C-NMR ($(CD_3)_2SO$) δ: 8.11 (q), 9.19 (q), 14.87 (q), 17.20 (t), 23.04 ('t'), 23.60 (t), 25.62 (t), 33.67/32.95 (dt, $^1J_{CC}$=55 Hz), 97.77 (d), 120.2 (s), 121.9 (s), 122.7 (s), 122.8 (s), 127.6 (s), 130.3 (s), 147.3 (s), 172.0 (s), 174.4 (s) ppm; HR-FAB-MS, calcd for $C_{33}{}^{13}C_2H_{44}N_4O_6$: 618.3328, found: 618.3302 amu.

Preparation of (n=4) [8⁵,12⁵-$^{13}C_2$]-Mesobilirubin-XIIIα (4). This rubin was prepared as outlined below using the procedures partly developed in the synthesis of **2**:[18,23,24,30]

3,5-Dimethyl-2-(methoxycarbonyl)-1H-pyrrole-3-butanoic Acid (29). As described for the preparation of **28**, **33** was saponified to **29** in 91% yield and used directly in the next step. It had mp 152-153°C; ^{1}H-NMR ($CDCl_3$) δ: 1.78 (2H, dt, J=7.3 Hz, 7.5 Hz), 2.20 (3H, s), 2.25 (3H, s), 2.35 (2H, t, J=7.3 Hz), 2.43 (2H, t, J=7.5 Hz), 3.82 (3H, s), 9.1 (1H, brs) ppm; ^{13}C-NMR ($CDCl_3$) δ: 10.63 (q), 11.45 (q), 23.19 (t), 25.43 (t), 33.21 (t), 51.02 (q), 116.6 (s), 120.8 (s), 127.4 (s), 130.5 (s), 162.5 (s), 179.1 (s) ppm; GC-MS (EI), *m/z*: 239 (30%) [$M^{+\bullet}$], 208 (10%) [M - OCH_3], 180 (10%) [M - CH_2CO_2H or M - CO_2CH_3], 166 (70%), [M - $CH_2CH_2CO_2H$], 134 (100%) amu.

Methyl 3,5-Dimethyl-4-(4-hydroxybutyl)-1H-pyrrole-2-carboxylate (26). As described above for **25**, **29** was converted to **26** in 96% yield and used directly in the next step. It had mp 103-104°C; ^{1}H-NMR ($CDCl_3$) δ: 1.52 (4H, m), 2.08 (1H, s), 2.18 (3H, s), 2.24 (3H, s), 2.37 (2H, t, J=7.2 Hz), 3.63 (2H, t, J=6.4 Hz), 3.81 (3H, s), 9.0 (1H, brs) ppm; ^{13}C-NMR ($CDCl_3$) δ: 10.59 (q), 11.45 (q), 23.68 (t), 26.87 (t), 32.33 (t), 50.83 (q), 62.79 (t), 116.4 (s), 121.8 (s), 127.1 (s), 129.9 (s), 162.3 (s) ppm; GC-MS (EI), *m/z*: 225 (30%) [$M^{+\bullet}$], 194 (15%) [M - OCH_3 or M - CH_2OH], 166 (90%) [M - CO_2CH_3 or M - $CH_2CH_2CH_2OH$], 134 (100%) amu.

Methyl 3,5-Dimethyl-4-(4-tosyloxybutyl)-1H-pyrrole-2-carboxylate (23). As described above for the 3-tosyloxypropyl analog (**22**), **23** was prepared from **26** in 83% yield and used directly in the next step. It had mp 83-85°C; ^{1}H-NMR ($CDCl_3$) δ: 1.40 (2H, m), 1.58 (2H, m), 2.12 (3H, s), 2.16 (3H, s), 2.29 (2H, t, J=7.4 Hz), 2.41 (3H, s), 3.78 (3H, s), 3.98 (2H, t, J=6.4 Hz), 7.74/7.30 (4H, AX, J=8.3 Hz), 8.8 (1H, brs) ppm; ^{13}C-NMR ($CDCl_3$) δ: 10.96 (q), 11.87 (q), 22.00 (q), 23.66 (t), 26.81 (t), 28.78 (t), 51.28 (q), 70.90 (t), 116.9 (s), 121.5 (s), 127.5 (s), 128.2 (d), 130.2 (d), 130.3 (s), 133.4 (s), 145.1 (s), 162.5 (s) ppm.

Methyl 3,5-Dimethyl-4-(4-^{13}CN cyanobutyl)-1H-pyrrole-2-carboxylate (20). As described for **19**, **23** was converted to **20** in 81% yield and used directly in the next step. It had mp 91.5-92.5°C; FT-IR (KBr) ν: 3311, 2946, 2928, 2860, 2193 (^{13}C≡N), 1677, 1453, 1373, 1272, 1190, 1101, 1080, 1000 cm^{-1}; ^{1}H-NMR ($CDCl_3$) δ: 1.61 (4H, m), 2.20 (3H, s), 2.25 (3H, s), 2.33 (2H, m), 2.40 (2H, t, J=7.4 Hz), 3.82 (3H, s), 8.6 (1H, brs) ppm; ^{13}C-NMR ($CDCl_3$) δ: 10.59 (q), 11.57 (q), 17.48/16.74 (dt, $^1J_{CC}$=56 Hz), 23.22 (t), 24.96 (t), 29.69 (t), 50.90 (q), 117.2 (s), 119.6 ("s"), 120.9 (s), 127.2 (s), 129.5 (s), 163.2 (s) ppm; GC-MS (EI) *m/z*: 235 (40%) [$M^{+\bullet}$], 204 (10%) [M - OCH_3], 166 (90%) [M - $CH_2CH_2CH_2{}^{13}C{\equiv}N$], 134 (100%) amu.

Methyl [8⁵-^{13}C]-2,7,9-Trimethyl-3-ethyl-(10H)-dipyrrinone-8-pentanoate (17). As described for the (n=2) xanthobilirubinate ester analog (**15**),[24,30] ^{13}C-labelled nitrile **20** was converted first to its diacid after saponification by heating in base for 36 hours, and then the diacid was converted directly to methyl (n=4)-xanthobilirubinate (**17**) in 63% yield. It had mp 177-178°C [Lit.[18] mp 177-178°C]; UV-vis: ε_{409}^{max} 31,700 ($CHCl_3$); FT-IR, ν: 3355, 2972, 2858, 1702, 1661, 1628, 1460, 1376, 1269, 1148 cm^{-1}; ^{1}H-NMR ($CDCl_3$) δ: 1.17 (3H, t, J=7.5 Hz), 1.47 (2H, m), 1.66 (2H, m), 1.94 (3H, s), 2.12 (3H, s), 2.32 (2H, dt, $^3J_{HH}$=7.8 Hz,

$^3J_{HC}$=7.5 Hz), 2.39 (3H, s), 2.40 (2H, t, J=8.0 Hz), 2.54 (2H, q, J=7.5 Hz), 3.66 (3H, d, $^3J_{CH}$= 3.7 Hz), 6.14 (1H, s), 10.3 (1H, brs), 11.3 (1H, brs) ppm; ^{13}C-NMR ($CDCl_3$) δ: 8.50 (q), 9.67 (q), 11.67 (q), 15.05 (q), 17.96 (t), 23.90 (t), 24.76 (t), 30.37 (dt, $^2J_{CC}$=3.2 Hz), 34.44/33.68 (dt, $^1J_{CC}$=57 Hz), 51.45 (dq, $^2J_{CC}$=2.3 Hz), 101.2 (d), 120.7 (s), 122.3 (2xs), 124.8 (s), 126.9 (s), 131.5 (s), 148.3 (s), 174.2 ("s"), 177.2 (s) ppm. It was used directly in the next step.

(n=4) [8^5,12^5-$^{13}C_2$]-Mesobiliverdin-XIIIα Dimethyl Ester (13). As reported for the synthesis of the (n=2) analog (**10**),[23,24] (n=4) [8^5-^{13}C]-xanthobilirubic acid methyl ester (**17**) was oxidatively coupled using *p*-chloranil to give the (n=4) verdin dimethyl ester (**13**) in 81% yield after flash chromatography. It had mp 168-170°C [lit.[18] mp 170-171°C]; UV-vis: ε_{369}^{max} 52,300, ε_{642}^{max} 15,300 ($CHCl_3$); FT-IR (KBr) ν: 3433, 3160, 2948, 2867, 1697, 1676, 1589, 1458, 1390, 1235, 1060 cm^{-1}; ^{1}H-NMR, δ: 1.21 (6H, t, J=7.5 Hz), 1.56 (4H, m), 1.69 (4H, m), 1.82 (6H, s) 2.06 (6H, s), 2.34 (4H, dt, $^3J_{HH}$=7.8 Hz, $^3J_{HC}$=7.5 Hz), 2.49 (4H, q, J=7.5 Hz), 2.59 (4H, t, J=7.5 Hz), 3.65 (6H, d, $^3J_{HC}$=3.7 Hz), 5.92 (2H, s), 6.61 (1H, s), 8.2 (3H, brs) ppm; ^{13}C-NMR, δ: 8.34 (q), 9.58 (q), 14.45 (q), 17.84 (t), 24.21 (t), 24.69 (t), 30.80 ('t'), 34.23/33.47 (dt, $^1J_{CC}$=57 Hz), 51.49 ('q'), 96.29 (d), 113.8 (d), 127.7 (s), 128.3 (s), 139.3 (s), 139.7 (s), 141.3 (s), 146.7 (s), 149.9 (s), 172.4 (s), 173.9 ('s') ppm. It was used directly in the next step.

(n=4) [8^5,12^5-$^{13}C_2$]-Mesobilirubin-XIIIα Dimethyl Ester (9). As described for the (n=2) rubin,[23,24] the corresponding (n=4) verdin (**13**) was reduced with $NaBH_4$ in 86% yield. It had mp 218-220°C [Lit.[18] mp 220-222°C]; UV-vis: ε_{380}^{max} 67,300, ε_{420}^{sh} 19,800 ($CHCl_3$); FT-IR (KBr) ν: 3358, 2968, 2936, 2865, 1697, 1663, 1636, 1458, 1364, 1172, 977 cm^{-1}; ^{1}H-NMR, δ: 1.00 (6H, t, J=7.5 Hz), 1.46 (6H, s), 1.56 (4H, m), 1.70 (4H, m), 2.08 (6H, s), 2.33 (8H, m), 2.53 (4H, t, J=7.5 Hz), 3.66 (6H, d, $^3J_{HC}$=3.5 Hz), 4.07 (2H, s), 5.91 (2H, s), 10.3 (2H, brs), 10.6 (2H, brs) ppm; ^{13}C-NMR, δ: 7.83 (q), 9.80 (q), 14.78 (q), 17.79 (t), 23.19 (t), 24.35 (t), 24.96 (t), 30.88 ('t'), 34.51/33.75 (dt, $^1J_{CC}$=58 Hz), 51.45 ('q'), 100.3 (d), 120.1 (s), 122.7 (s), 123.4 (s), 123.7 (s), 128.7 (s), 130.8 (s), 146.9 (s), 173.9 (s), 174.2 ('s') ppm. It was used directly in the next step.

(n=4) [8^5,12^5-$^{13}C_2$]-Mesobilirubin-XIIIα (4). As described for (n=2)[8^3,12^3-$^{13}C_2$]-mesobilirubin-XIIIα (**2**),[18,24] the (n=4) rubin dimethyl ester (**9**) was saponified to afford rubin **4** in 82% crude yield, 56% yield after recrystallization. It had mp 228-231°C [lit[18] mp 230-233°C]; UV-vis: ε_{428}^{max} 39,300, ε_{398}^{sh} 32,000 ($(CH_3)_2SO$); FT-IR (KBr) ν: 3346, 2966, 2934, 2867, 1664, 1637, 1458, 1364, 1172, 978 cm^{-1}; ^{1}H-NMR ($(CD_3)_2SO$), δ: 0.99 (4H, m), 1.04 (6H, t, $^3J_{HH}$=7.5 Hz), 1.29 (4H, m), 1.74 (6H, s), 1.95 (6H, s), 2.00 (4H, 'q'), 2.10 (4H, t, $^3J_{HH}$=7.5 Hz, $^3J_{HC}$=7.3 Hz), 2.45 (4H, q, J=7.5 Hz), 3.89 (2H, s), 5.92 (2H, s), 9.8 (2H, brs), 10.3 (2H, brs), 11.8 (2H, brs) ppm; ^{13}C-NMR ($(CD_3)_2SO$) δ: 8.38 (q), 9.47 (q), 15.11 (q), 17.47 (t), 23.83 (t), 24.08 (t), 24.92 (t), 30.10 ('t'), 34.26/33.52 (dt, J_{CC}=55 Hz), 97.94 (d), 121.0 (s), 122.0 (s), 123.0 (2xs), 127.8 (s), 130.6 (s), 147.5 (s), 172.2 (s), 174.7 ('s') ppm; HR-FAB MS, calcd for $C_{35}{}^{13}C_2H_{48}N_4O_6$: 646.3640, found: 646.3632 amu.

[8^3,12^3 - $^{13}C_2$]-10,10-Dimethylglaucorubin (**5**) was prepared as described previously.[20,23]

Acknowledgements: We thank the National Institutes of Health (HD 17779) for generous support and the National Science Foundation (CHE-9214294) for assistance in purchasing the 500 MHz NMR spectrometer used in this work. Special thanks go to Dr. Darren Holmes for preparing compounds **1** and **5** and to Mr. Lew Cary for his assistance in the NMR experiments.

REFERENCES

1. McDonagh, A.F. *Bile Pigments: Bilatrienes and 5,15-Biladienes.* In *The Porphyrins*; Dolphin, D., Ed.; Academic Press: New York, **1979**, *6*, 293.

2. Schmid, R.; McDonagh, A.F. Hyperbilirubinemia. In *The Metabolic Basis for Inherited Diseases* (Stanbury, J.B.; Wyngaarden, J.B.; Frederickson, D.S., Eds.), McGraw-Hill: NY, 1978, pp. 1221-57.
3. Chowdury, J.R., Wolkoff, A.W., Chowdury, N.R., and Arias, I.M. "Hereditary Jaundice and Disorders of Bilirubin Metabolism" in *The Metabolic and Molecular Bases of Inherited Disease* (Scriver, C.R., Beaudet, A.L., Sly, W.S., and Valle, D., eds.) McGraw-Hill, Inc., New York, *Vol. II*, 1995, chap. 67, 2161-2208.
4. Neuzil, J.; Stocker, R. *J. Biol. Chem.*, **1994**, *269*, 16712-16719.
5. Berk, P.D.; Noyer, C. *Seminars Liver Dis.*, **1994**, *14*, 323-394.
6. Bonnett, R.; Davies, J. E.; Hursthouse, M. B.; Sheldrick, G. M. *Proc. R. Soc. London, Ser. B*, **1978**, *202*, 249-268.
7. LeBas, G.; Allegret, A.; Mauguen, Y.; DeRango, C.; Bailly, M. *Acta Crystallogr., Sect. B*, **1980**, *B36*, 3007-3011.
8. Person, R.V.; Peterson, B.R.; Lightner, D.A. *J. Am. Chem. Soc.*, **1994**, *116*, 42-59.
9. Lightner, D.A.; Person, R.V.; Peterson, B.R.; Puzicha, G.; Pu, Y-M.; Boiadjiev, S. *Biomolecular Spectroscopy II* (Birge, R.R.; Nafie, L.A., eds.), Proc. SPIE *1432*, **1991**, 2-13.
10. Shelver, W.H.; Rosenberg, H.; Shelver, W.H. *Intl. J. Quantum Chem.*, **1992**, *44*, 141-163.
11. Shelver, W.L.; Rosenberg, H.; Shelver, W.H. *J. Molec. Struct.*, **1994**, *312*, 1-9.
12. Mugnoli, A.; Manitto, P.; Monti, D. *Acta Crystallogr., Sect. C*, **1983**, *39*, 1287-1291.
13. Kaplan, D.; Navon, G. *Israel J. Chem.* **1983**, *23*, 177-186.
14. Pu, Y.M.; Lightner, D.A. *Tetrahedron* **1991**, *47*, 6163-6170.
15. Nogales, D.; Lightner, D.A. *J. Biol. Chem.* **1995**, *270*, 73-77.
16. Boiadjiev, S.E.; Person, R.V.; Puzicha, G.; Knobler, C.; Maverick, E.; Trueblood, K.N.; Lightner, D.A. *J. Am. Chem. Soc.* **1992**, *114*, 10123-10133.
17. Navon, G.; Frank, S.; Kaplan, D. *J. Chem. Soc., Perkin Trans. 2* **1984**, 1145-1149.
18. Shrout, D.P.; Puzicha, G.; Lightner, D.A. *Synthesis* **1992**, 328-332.
19. Person, R.V. *Conformational Analysis of Bilirubin and Its Analogs*, Ph.D. Dissertation, University of Nevada, 1993.
20. Xie, M.; Lightner, D.A. *Tetrahedron* **1993** *49*, 2185-2200.
21. Neuhaus, D.; Williamson, M.P. *The Nuclear Overhauser Effect in Structural and Conformational Analysis*, VCH Publishers, 1989.
22. Kövér, K.E.; Bata, G. *Progress in NMR Spectroscopy*, **1987**, *19*, 223-266.
23. Holmes, D.L.; Lightner, D.A. *Tetrahedron* **1996**, *52*, 5319-5338.
24. Nogales, D.; Lightner, D.A. *J. Labelled Cpds & Radiopharm.* **1994**, *34*, 453-462.
25. Kaplan, D.; Navon, G. *J. Chem. Soc. Perkin Trans 2* **1981**, 1364-1383.
26. Falk, H. *The Chemistry of Linear Oligopyrroles and Bile Pigments*; Springer Verlag: New York/Wien, 1989.
27. Carey, M.C.; Spivak, W. "Physical Chemistry of Bile Pigments and Porphyrins" in *Bile Pigments and Jaundice* (Ostrow, J.D., ed.), Marcel Dekker, New York, 1986, pp 81-132.
28. Lightner, D.A. "Structure, Photochemistry and Organic Chemistry of Bilirubin" in *Bilirubin* (Heirwegh, K.P.M.; Brown, S.B., eds.), Vol I, CRC Press, Boca Raton, FL, 1982, pp 1-58.
29. Kaplan, D.; Navon, G. *Biochem. J.* **1982**, *201*, 605-613.
30. Holmes, D.L.; Lightner, D.A. *Tetrahedron* **1995**, *51*, 1607-1622.
31. Puzicha, G.; Shrout, D.P.; Lightner, D.A. *J. Heterocyclic Chem.* **1990**, *27*, 2117-2123.

(*Received in USA* 25 *October* 1996; *revised* 27 *December* 1996; *accepted* 8 *January* 1997)